The relationship between the distribution of electronic states and the optical absorption spectrum of an amorphous semiconductor: An empirical analysis

Stephen K. O'Leary[a)]
Department of Electrical, Computer, and Systems Engineering, Rensselaer Polytechnic Institute, Troy, New York 12180-3590 and Department of Physics, Hong Kong Baptist University, Kowloon Tong, Kowloon, Hong Kong

S. R. Johnson
Center for Solid State Electronics Research, Arizona State University, Box 876206, Tempe, Arizona, 85287-6206

P. K. Lim
Department of Physics, Hong Kong Baptist University, Kowloon Tong, Kowloon, Hong Kong

(Received 16 December 1996; accepted for publication 24 June 1997)

An elementary empirical model for the distribution of electronic states of an amorphous semiconductor is presented. Using this model, we determine the functional form of the optical absorption spectrum, focusing our analysis on the joint density of states function, which dominates the absorption spectrum over the range of photon energies we consider. Applying our optical absorption results, we then determine how the empirical measures commonly used to characterize the absorption edge of an amorphous semiconductor, such as the Tauc gap and the absorption tail breadth, are related to the parameters that characterize the underlying distribution of electronic states. We, thus, provide the experimentalist with a quantitative means of interpreting the physical significance of their optical absorption data. © *1997 American Institute of Physics.* [S0021-8979(97)02919-8]

I. INTRODUCTION

Optical absorption in amorphous semiconductors continues to be the focus of considerable study. In a defect-free crystalline semiconductor, the absorption spectrum terminates abruptly at the energy gap. In contrast, in an amorphous semiconductor, a tail in the absorption spectrum encroaches into the gap region.[1] This tail in the absorption spectrum makes the absorption edge of an amorphous semiconductor difficult to define experimentally. As a consequence, various empirical measures for the optical gap and the absorption tail breadth have been devised. While these empirical measures facilitate the quantitative analysis of the absorption edge, their physical meaning has yet to be clearly established.

In order to provide a proper theoretical basis for the interpretation of the optical absorption spectrum of amorphous semiconductors, the distribution of electronic states must be known. While the distribution of states of a defect-free crystalline semiconductor terminates abruptly at the band edge, in an amorphous semiconductor a distribution of tail states encroaches into the otherwise empty gap region.[2] Analysis shows that many of these tail states are localized by the site disorder, and that there exists a critical energy, termed the mobility edge, which separates localized states from their extended counterparts.[3,4] These localized states are responsible for many of the unique properties exhibited by amorphous semiconductors.

In this paper, we employ an elementary empirical model for the distribution of electronic states and determine the corresponding optical absorption spectrum within the framework of this model. Our goal is to establish a clear relationship between the form of the optical absorption spectrum and the form of the distribution of electronic states. In particular, we determine how the empirical measures commonly used to characterize the absorption edge of an amorphous semiconductor are related to the parameters that characterize the underlying distribution of electronic states. We, thus, provide the experimentalist with a means of interpreting the physical significance of their optical absorption data.

This paper is organized in the following manner. In Sec. II, we present our elementary empirical model for the distribution of electronic states, focusing on the one-electron density-of-states (DOS) function $N(E)$, $N(E)\Delta E$ representing the number of one-electron states, per unit volume, between energies $[E,E+\Delta E]$. Then, in Sec. III, we use this model to determine the functional form of the optical absorption spectrum. The relationship between the form of the optical absorption spectrum and the form of the distribution of electronic states is discussed in Sec. IV. Finally, conclusions are presented in Sec. V.

II. MODELING THE DISTRIBUTION OF ELECTRONIC STATES

Theoretical analyses of the distribution of electronic states in amorphous semiconductors have a long and rich tradition. Traditionally, the distribution of tail states has been attributed to the distribution of potential fluctuations.[5–9] However, Zhang and Sheng[10] pointed out that there are experimentally observed features in the tail, which are not explainable solely on the basis of random potential fluctuations,

a)Electronic Mail: oleary@ecse.rpi.edu

 0021-8979/97/82(7)/3334/7/$10.00

suggesting that other physical mechanisms are at play as well. Silver and co-workers[11,12] demonstrated that the interaction between localized states and the charges, which are randomly distributed throughout these semiconductors, influences the distribution of tail states considerably. O'Leary *et al.*[13,14] showed that phase heterogeneities also influence the tail. Thus, at present, even the origin of the distribution of tail states remains unresolved.

In order to bypass this theoretical conundrum, we adopt an elementary empirical model for the distribution of electronic states, which captures the basic expected features. It is now widely recognized that the distribution of states exhibits a square-root functional dependence in the band region and an exponential functional dependence in the tail region, although the exact form of the tail is still the subject of considerable controversy.[15–25] It is also known that the transition in the DOS function between the band region and the tail region is a smooth one.[21,23,25] Thus, we assume that the conduction-band DOS function

$$N_c(E)=\frac{\sqrt{2}m_c^{*3/2}}{\pi^2\hbar^3}\begin{cases}\sqrt{E-V_c}, & E\geqslant V_c+\dfrac{\gamma_c}{2}\\ \sqrt{\dfrac{\gamma_c}{2}}\exp\left(-\dfrac{1}{2}\right)\exp\left(\dfrac{E-V_c}{\gamma_c}\right), & \\ E<V_c+\dfrac{\gamma_c}{2}\end{cases} \tag{1}$$

where m_c^* represents a DOS effective mass which we associate with the conduction band, V_c denotes the conduction-band disorderless band edge, γ_c reflects the breadth of the conduction-band tail, and $V_c+\gamma_c/2$ denotes the transition point between square-root and linear-exponential distributions of states, $N_c(E)$ and its first derivative being continuous at this point.[26] Similarly, we assume that the valence-band DOS function

$$N_v(E)=\frac{\sqrt{2}m_v^{*3/2}}{\pi^2\hbar^3}\begin{cases}\sqrt{\dfrac{\gamma_v}{2}}\exp\left(-\dfrac{1}{2}\right)\exp\left(\dfrac{V_v-E}{\gamma_v}\right), & \\ E\geqslant V_v-\dfrac{\gamma_v}{2} & \\ \sqrt{V_v-E}, & E<V_v-\dfrac{\gamma_v}{2}\end{cases}, \tag{2}$$

where m_v^* represents a DOS effective mass, which we associate with the valence band, V_v denotes the valence- band disorderless band edge, γ_v reflects the breadth of the valence-band tail, and $V_v-\gamma_v/2$ denotes the transition point between square-root and linear-exponential distributions of states, $N_v(E)$ and its first derivative being continuous at this point. Despite the controversy concerning the exact form of the distribution of tail states, as most experiments are interpreted in terms of a linear-exponential distribution of tail states, there is a certain amount of theoretical raison d'être for employing a linear-exponential distribution of tail states in our analysis. As the band tailing, which occurs in amorphous semiconductors, is fundamentally related to the disorder that characterizes these materials, the tail breadth parameters, γ_c and γ_v, provide a measure of this disorder. Assuming that all tail states are localized and all band states are extended, we suggest that the energy levels $V_c+\gamma_c/2$ and $V_v-\gamma_v/2$ represent the mobility edges of the conduction and valence bands, respectively.

To study the effect of disorder, we examine the sensitivity of $N_c(E)$ to variations in γ_c. In Fig. 1, we plot this DOS function for a number of selections of γ_c, m_c^* being set to the free-electron mass m_e. In the disorderless limit, where $\gamma_c\rightarrow 0$, we see that the conduction-band DOS function terminates abruptly at the disorderless band edge V_c, i.e.,

$$N_c(E)\rightarrow\frac{\sqrt{2}m_c^{*3/2}}{\pi^2\hbar^3}\begin{cases}\sqrt{E-V_c}, & E\geqslant V_c\\ 0, & E<V_c\end{cases}. \tag{3}$$

In contrast, for finite γ_c, a distribution of tail states appears below the mobility edge. As γ_c increases from this disorderless limit, the total number of localized tail states increases, and the distribution of tail states further encroaches into the gap. Similar results are also observed for the valence-band DOS function $N_v(E)$.

We now demonstrate that our elementary empirical model for the distribution of electronic states is consistent with experiment. In Fig. 2(a), we plot the conduction-band DOS results of Longeaud and Vanderhaghen,[24] derived from time-of-flight measurements of high-quality hydrogenated amorphous silicon. Setting m_c^* equal to $1.08m_e$, this being the conduction-band DOS effective mass associated with crystalline silicon,[27] we find that the selection of γ_c between 25 and 30 meV leads to a distribution of electronic states, which is reasonably consistent with these experimental results, within the range of experimental error. Other experimental determinations of the breadth of the conduction-band tail have come to similar conclusions.[28] It should be noted, however, that deep in the tail (below -200 meV) there are deviations, which occur between our modeling result and the experimental results of Longeaud and Vanderhaghen,[24] sug-

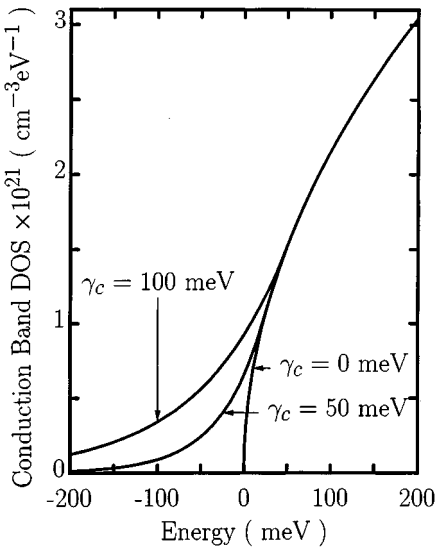

FIG. 1. The conduction-band DOS function $N_c(E)$ corresponding to various selections of γ_c. The conduction-band disorderless band-edge V_c is set equal to zero in all cases.

gesting that the distribution of conduction-band tail states of high-quality hydrogenated amorphous silicon is not exactly linear-exponential in form.

In Fig. 2(b), we plot the valence-band DOS results of Winer and Ley,[21] these results being derived from total-yield photoelectron spectroscopy measurements of high-quality hydrogenated amorphous silicon. Setting m_v^* equal to 0.56 m_e, this being the valence-band DOS effective mass associated with crystalline silicon,[27] we find that the selection of γ_v between 40 and 50 meV leads to a distribution of electronic states, which is reasonably consistent with these experimental results, within the range of experimental error. Other experimental determinations of the breadth of the valence-band tail have come to similar conclusions.[29] It should be noted, however, that deep in the tail (above 400 meV) and high in the band (below -100 meV), there are deviations that occur between our modeling result and the experimental results of Winer and Ley.[21] Winer and Ley[21] suggest that the deep tail structure arises as a consequence of the distribution of deep gap states, these not being considered in our model for the distribution of electronic states. The high-energy deviations may be attributed to an artifact of the experimental methodology of Winer and Ley;[21] Winer and Ley[21] determined the valence-band DOS function $N_v(E)$ from the results of total-yield photoelectron spectroscopy measurements assuming that $N_c(E)$ was constant, and thus, an overestimation of $N_v(E)$ may arise.

III. OPTICAL ABSORPTION IN AMORPHOUS SEMICONDUCTORS

In an amorphous semiconductor, momentum is a poor quantum number. As a result, only energy conservation need be satisfied for a successful optical transition. This being the case, it can be shown that the optical absorption coefficient

$$\alpha(\hbar\omega)=D^2(\hbar\omega)J(\hbar\omega), \tag{4}$$

where $J(\hbar\omega)$ denotes the joint density-of-states (JDOS) function, $D^2(\hbar\omega)$ being the optical transition matrix element.[30–33] At low temperatures, in the undoped or lightly doped case, assuming independent conduction-band and valence-band potential fluctuations,[34] this JDOS function may be expressed as

$$J(\hbar\omega)=\int_{-\infty}^{\infty} N_c(E)N_v(E-\hbar\omega)dE. \tag{5}$$

In order to facilitate our analysis, we introduce the normalized JDOS function,

$$\mathscr{J}(\hbar\omega)\equiv\frac{\pi^2\hbar^3}{\sqrt{2}m_c^{*3/2}}\frac{\pi^2\hbar^3}{\sqrt{2}m_v^{*3/2}}J(\hbar\omega), \tag{6}$$

defined such that

$$\alpha(\hbar\omega)=D^2(\hbar\omega)\frac{\sqrt{2}m_c^{*3/2}}{\pi^2\hbar^3}\frac{\sqrt{2}m_v^{*3/2}}{\pi^2\hbar^3}\mathscr{J}(\hbar\omega). \tag{7}$$

The exact functional dependence of $D^2(\hbar\omega)$ remains unknown. The analysis of Hindley[35] suggests that $D^2(\hbar\omega)$ should exhibit a relatively smooth functional dependence for the extended-state-to-extended-state optical transitions, the extended-state-to-localized-state optical transitions, and the localized-state-to-extended-state optical transitions. However, Hindley also predicts a sudden and dramatic reduction in the magnitude of $D^2(\hbar\omega)$ for the localized-state-to-localized-state optical transitions. Variations in the magnitude of the optical transition matrix element have been observed experimentally by Jackson *et al.*,[32] however, the existence of a sharp discontinuity in the functional dependence of $D^2(\hbar\omega)$ has yet to be experimentally confirmed. Given the uncertainty in the functional dependence of the optical transition matrix element, we feel that our analysis is

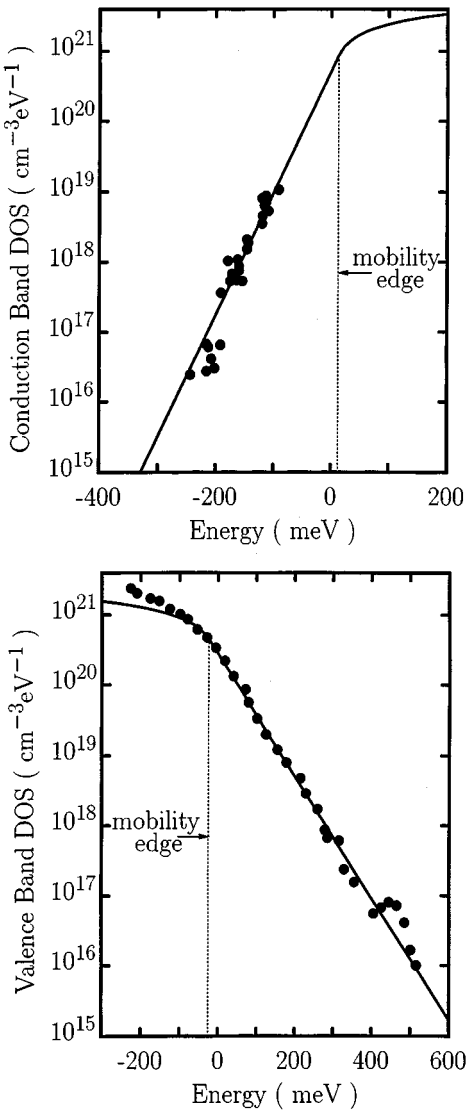

FIG. 2. (a)The conduction-band DOS function $N_c(E)$. The experimental data of Longeaud and Vanderhaghen (Fig. 5 of Ref. 24) is represented with the solid points. Our modeling result is represented by the solid line; $\gamma_c=25$ meV and $V_c=0$ meV. The mobility edge is represented by the light dotted line; this edge is at energy-level $V_c+\gamma_c/2$. (b) The valence-band DOS function $N_v(E)$. The experimental data of Winer and Ley (Fig. 7 of 21) is represented with the solid points. Our modeling result is represented by the solid line; $\gamma_v=50$ meV and $V_v=0$ meV. The mobility edge is represented by the light dotted line; this edge is at energy-level $V_v-\gamma_v/2$.

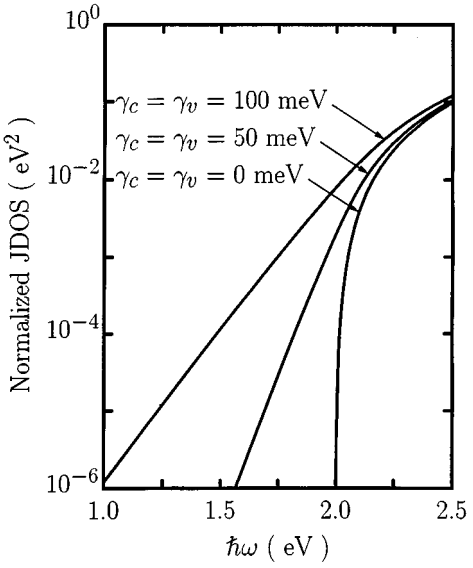

FIG. 3. The normalized joint density-of-states function $\mathcal{J}(\hbar\omega)$ corresponding to various selections of γ_c and γ_v. The disorderless Tauc gap E_{g_o} is set to 2 eV in all cases.

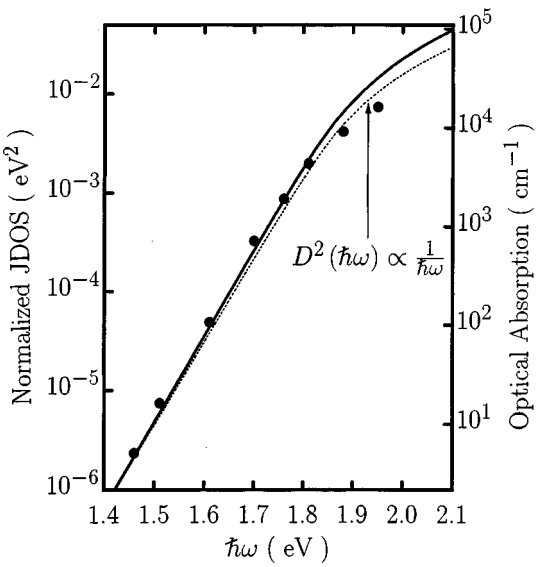

FIG. 4. Optical absorption: a comparison with experiment. The experimental data of Roxlo *et al.* (Ref. 44) is represented with the solid points (Fig. 2 of Ref. 44). Our modeling result is represented by the solid line; $E_{g_o}=1.78$ eV, $\gamma_c=25$ meV, and $\gamma_v=50$ meV. The scaling between $\alpha(\hbar\omega)$ and $\mathcal{J}(\hbar\omega)$, $\alpha(\hbar\omega)=2.2\times10^6\mathcal{J}(\hbar\omega)$, is consistent with that of Jackson *et al.* (Ref. 32). In order to demonstrate that the deviation, which occurs at higher photon energies (above 1.8 eV), is due to our neglect of the functional form of the optical transition matrix element $D^2(\hbar\omega)$, we make the usual assumption that $D^2(\hbar\omega)\propto 1/\hbar\omega$, and multiply this by $\mathcal{J}(\hbar\omega)$, normalizing at $\hbar\omega=1.4$ eV. The resultant curve is depicted with the light dotted line.

best served by following the lead of Grein and John,[36] and focusing on the determination of the functional properties of $\mathcal{J}(\hbar\omega)$.

We first consider the form of $\mathcal{J}(\hbar\omega)$ in the disorderless limit, i.e., as $\gamma_c\rightarrow 0$ and $\gamma_v\rightarrow 0$. Noting, from Eq. (2), that in the disorderless limit,

$$N_v(E)\rightarrow \frac{\sqrt{2}m_v^{*3/2}}{\pi^2\hbar^3}\begin{cases}0, & E>V_v\\ \sqrt{V_v-E}, & E\leqslant V_v\end{cases}, \tag{8}$$

we see, from Eqs. (3), (5), (6), and (8), that

$$\mathcal{J}(\hbar\omega)\rightarrow\begin{cases}\dfrac{\pi}{8}(\hbar\omega-E_{g_o})^2, & \hbar\omega\geqslant E_{g_o}\\ 0, & \hbar\omega<E_{g_o}\end{cases}, \tag{9}$$

where

$$E_{go}\equiv V_c-V_v\,. \tag{10}$$

This parabolic absorption edge, arising as a consequence of optical transitions between square-root bands, is referred to as the Tauc absorption edge,[37–42] E_{g_o} being the value of the Tauc gap in the disorderless limit.

We now introduce the effect of disorder. In Fig. 3, we plot the functional dependence of $\mathcal{J}(\hbar\omega)$ over a broad range of photon energies, for a number of selections of γ_c and γ_v, E_{g_o} being held at 2 eV. We note that with the introduction of disorder, a tail in the absorption spectrum encroaches into the gap region, the breadth of this absorption tail increasing with the amount of disorder, as observed experimentally by Cody *et al.*[43] We further note that $\mathcal{J}(\hbar\omega)$ exhibits a smooth transition from below to above the mobility gap, $E_{g_o}+\gamma_c/2+\gamma_v/2$, the mobility gap denoting the energy difference between conduction-band and valence-band mobility edges. Analytical expressions for the normalized JDOS function are developed in the Appendix.

To demonstrate that our JDOS results are consistent with experiment, in Fig. 4 we plot the high-quality hydrogenated amorphous silicon optical absorption data of Roxlo *et al.*[44] These results have been scaled to facilitate a comparison with $\mathcal{J}(\hbar\omega)$, the scaling between $\alpha(\hbar\omega)$ and $\mathcal{J}(\hbar\omega)$ being consistent with that of Jackson *et al.*[32] Alongside, we plot our modeling result for the parameter selections $E_{g_o}=1.78$ eV, $\gamma_c=25$ meV, and $\gamma_v=50$ meV, noting that these selections are consistent with the results of our previous analysis, i.e., Figs. 2(a) and 2(b). We see that our modeling result is reasonably consistent with the experimental results of Roxlo *et al.*,[44] within the range of experimental error. The discrepancy between $\alpha(\hbar\omega)$ and $\mathcal{J}(\hbar\omega)$, observed at higher photon energies (above 1.8 eV), may be attributed to our neglect of the optical transition matrix element $D^2(\hbar\omega)$. If we assume that the momentum matrix element is constant, implying that $D^2(\hbar\omega)\propto 1/\hbar\omega$,[37–41] as is commonly assumed in the literature, we see that the discrepancy disappears.

IV. DISCUSSION

We now relate the empirical measures commonly used to characterize the absorption edge of an amorphous semiconductor with the parameters used to characterize the distribution of electronic states. The optical gap is usually determined through the analysis of Tauc and co-workers,[37,38] in which an extrapolation of the apparent linear functional dependence of $\sqrt{\alpha(\hbar\omega)/D^2(\hbar\omega)}$, observed in amorphous semiconductors at sufficiently large values of $\hbar\omega$, is used to define a gap, referred to as the Tauc gap $E_{g_{\text{Tauc}}}$. In Fig. 5, we

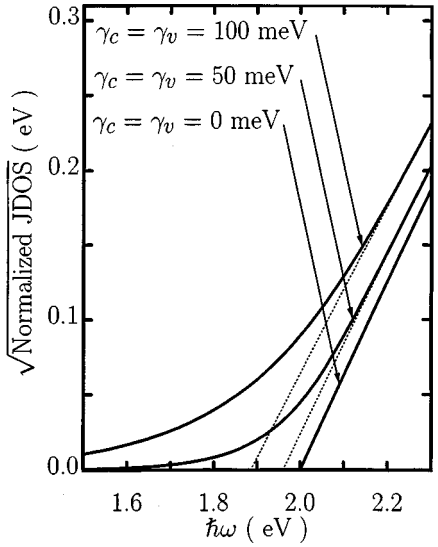

FIG. 5. The square root of the normalized joint density-of-states function $\mathcal{J}(\hbar\omega)$. The disorderless Tauc gap E_{g_o} is set to 2 eV in all cases. We note that the Tauc gaps $E_{g_{\text{Tauc}}}$, determined by extrapolating the apparent linear dependence of $\sqrt{\mathcal{J}(\hbar\omega)}$ observed at sufficiently large values of $\hbar\omega$, are found to be 2.00, 1.96, and 1.89 eV for the cases of $\gamma_c = \gamma_v$ equal to 0, 50, and 100 meV, respectively. The extrapolations used to determine these Tauc gaps are depicted by the light dotted lines.

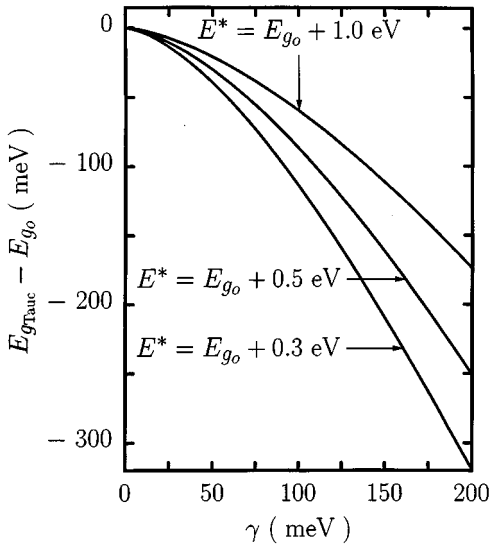

FIG. 6. The variation of the Tauc gap $E_{g_{\text{Tauc}}}$ with γ, for the case of $\gamma_c = \gamma_v = \gamma$. In order for this plot to be independent of any particular selection of E_{g_o}, the abscissa is actually the difference between $E_{g_{\text{Tauc}}}$ and E_{g_o}. In order to determine the role that E^* plays in these results, we plot this relationship for a number of selections of E^*, E^* denoting the photon energy where $\sqrt{\mathcal{J}(\hbar\omega)}$ is linearized.

plot $\sqrt{\mathcal{J}(\hbar\omega)}$ for a number of selections of γ_c and γ_v, E_{g_o} being set equal to 2 eV. It is seen that for high energies, in all cases, $\sqrt{\mathcal{J}(\hbar\omega)}$ exhibits an essentially linear functional dependence on $\hbar\omega$, i.e., Tauc absorption edges are observed. Extrapolating this high-energy Tauc absorption behavior to zero absorption, it is seen that $E_{g_{\text{Tauc}}}$ decreases monotonically from E_{g_o} as the disorder is increased, even though E_{g_o} remains fixed; as $\sqrt{\mathcal{J}(\hbar\omega)}$ does not exhibit an exactly linear functional dependence, we actually linearized $\sqrt{\mathcal{J}(\hbar\omega)}$ at the photon energy $E^* = 2.3$ eV, and used that linearization to determine $E_{g_{\text{Tauc}}}$. This result demonstrates that $E_{g_{\text{Tauc}}}$ is not simply equal to the difference between V_c and V_v, as might have been expected from the analysis of Tauc and co-workers.[37,38] Rather, the disorder parameters, γ_c and γ_v, are also seen to play a role in determining the magnitude of $E_{g_{\text{Tauc}}}$.

In Fig. 6, we plot the relationship between $E_{g_{\text{Tauc}}}$, E_{g_o}, γ_c, and γ_v, focusing on the case of $\gamma_c = \gamma_v = \gamma$. As observed in Fig. 5, in all cases $E_{g_{\text{Tauc}}}$ decreases in response to increases in γ. In order to assess the sensitivity of $E_{g_{\text{Tauc}}}$ to where the linearization of $\sqrt{\mathcal{J}(\hbar\omega)}$ is performed, we evaluate the functional dependence of $E_{g_{\text{Tauc}}}$ on γ for three different selections of E^*, spanning over the usual range of experimental analyses, E^* denoting the photon energy at which $\sqrt{\mathcal{J}(\hbar\omega)}$ is linearized. We find that, when γ is fixed, $E_{g_{\text{Tauc}}}$ increases with E^*, suggesting that the slope of $\sqrt{\mathcal{J}(\hbar\omega)}$ increases with $\hbar\omega$. Uncertainty in the determination of $E_{g_{\text{Tauc}}}$ due to questions as to where one should linearize $\sqrt{\mathcal{J}(\hbar\omega)}$ often occurs experimentally; see, for example, Kruzelecky *et al.*[40] This plot provides a quantitative means of reducing this uncertainty.

In an amorphous semiconductor, the absorption tail is often assumed to exhibit a linear-exponential functional dependence on the photon energy, i.e.,

$$\alpha(\hbar\omega) = \alpha_o \exp\left(\frac{\hbar\omega - \hbar\omega_o}{E_o}\right), \tag{11}$$

where α_o and $\hbar\omega_o$ are numerical constants, and E_o is referred to as the absorption tail breadth.[42,43] The absorption tail breadth parameter is yet another parameter, which is commonly used to characterize the absorption edge of an amorphous semiconductor. Our JDOS results are essentially linear exponential in form in the tail region, and thus, an analysis of E_o may be readily facilitated; in actual fact, there is some departure from the linear-exponential dependence of $\alpha(\hbar\omega)$ on $\hbar\omega$, as was demonstrated experimentally by Roxlo *et al.*,[44] and thus, following the suggestion of Persans *et al.*,[45] E_o may be more generally defined by taking the inverse of the logarithmic slope of $\alpha(\hbar\omega)$, i.e.,

$$E_o \equiv \left[\frac{d \ln \alpha(\hbar\omega)}{d\hbar\omega}\right]^{-1}. \tag{12}$$

In order to study how the absorption tail breadth E_o depends on the modeling parameters, in Fig. 7 we plot the functional dependence of $\mathcal{J}(\hbar\omega)$ over a broad range of photon energies, for number of selections of γ_v, γ_c being held at 100 meV and E_{g_o} being set to 2 eV. When $\gamma_v = 0$ meV, the absorption tail breadth is exclusively governed by the breath of the conduction-band tail, and $E_o = 100$ meV. As γ_v is increased, however, while the magnitude of the absorption tail is increased, the breadth of the absorption tail remains essentially unchanged until γ_v exceeds 100 meV, in which case E_o starts to increase almost linearly with γ_v. Owing to

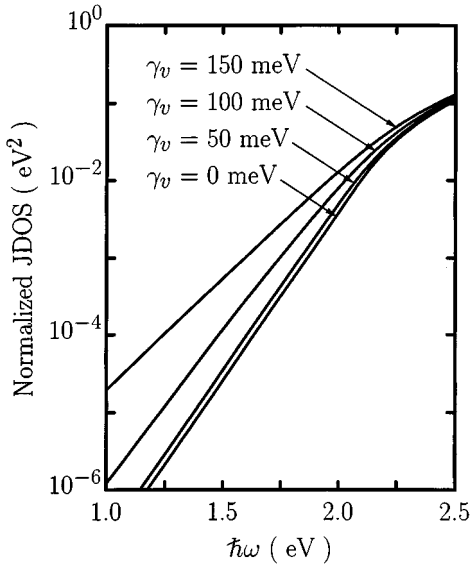

FIG. 7. The normalized joint density of states function $\mathscr{J}(\hbar\omega)$. The disorderless Tauc gap E_{g_o} is set to 2 eV in all cases. γ_c is set to 100 meV in all cases.

the symmetry in the relationship between γ_c and γ_v and the JDOS function, this result suggests that E_o is dominated by the maximum of γ_c and γ_v, i.e.,

$$E_o \sim \mathrm{Max}(\gamma_c, \gamma_v). \tag{13}$$

In order to assess this relationship in a more quantitative manner, we plot the variation of E_o with γ_v, γ_c being held at 100 meV, in Fig. 8; to determine E_o, we adopt the suggestion of Persans *et al.*,[45] i.e.,

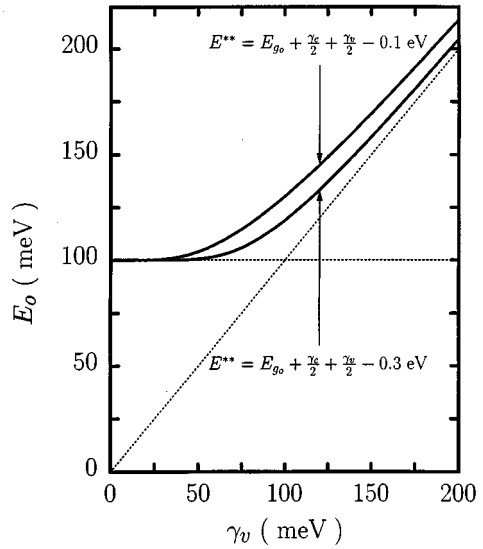

FIG. 8. The absorption tail breadth as a function of γ_v, for the case of γ_c being set to 100 meV; the value of E_{g_o} does not need to be specified. We determine E_o using Eq. (14) for two selections of E^{**}; (1) $E^{**} = E_{g_o} + \gamma_c/2 + \gamma_v/2 - 0.1$ eV, and (2) $E^{**} = E_{g_o} + \gamma_c/2 + \gamma_v/2 - 0.3$ eV, these spanning over the usual experimental range, $E_{g_o} + \gamma_c/2 + \gamma_v/2$ denoting the mobility gap. The dotted lines represent γ_c and γ_v, respectively.

$$E_o \equiv \left[\frac{d \ln \mathscr{J}(\hbar\omega)}{d\hbar\omega} \right]^{-1} \Bigg|_{\hbar\omega = E^{**}}, \tag{14}$$

where E^{**} denotes the photon energy at which this inverse logarithmic derivative is evaluated. We note that, as was observed in Fig. 7, the absorption tail breadth remains relatively constant until γ_v exceeds γ_c, in which case it increases essentially linearly with γ_v. The expression in Eq. (13) is seen to form a lower bound on our numerical results. The variation of E_o with E^{**}, γ_v being fixed, is seen to be in the range specified by Roxlo *et al.*[46]

V. CONCLUSIONS

In conclusion, we have used an elementary empirical model for the distribution of electronic states to determine the form of the optical absorption spectrum. Applying our optical absorption results, we determined how the Tauc gap and the absorption tail breadth are related to the parameters that characterize the underlying distribution of electronic states. We have, thus, developed a means by which an experimentalist will be able to relate the parameters commonly used to characterize the optical absorption spectrum of an amorphous semiconductor with those used to characterize the corresponding distribution of electronic states.

ACKNOWLEDGMENTS

The authors wish to thank Dr. C. Aversa, of the University of California at Santa Barbara, for some useful and helpful discussions. The contributions of Professor T. Tiedje, of the University of British Columbia, and Professor J. M. Perz and Professor S. Zukotynski, both of the University of Toronto, are also noted. Financial assistance from the Hong Kong Baptist University and the administrative assistance of T. Y. Leung is gratefully acknowledged. One of the authors (S.K.O.) wishes to acknowledge support from a Natural Sciences and Engineering Research Council of Canada Postdoctoral Fellowship.

APPENDIX: ANALYTICAL EXPRESSIONS FOR THE JDOS FUNCTION

The analysis of the JDOS function naturally divides into two regimes; (1) $\hbar\omega \leqslant E_{g_o} + \gamma_c/2 + \gamma_v/2$, and (2) $\hbar\omega \geqslant E_{g_o} + \gamma_c/2 + \gamma_v/2$, where $E_{g_o} + \gamma_c/2 + \gamma_v/2$ denotes the mobility gap. For the case of $\hbar\omega \leqslant E_{g_o} + \gamma_c/2 + \gamma_v/2$, from Eqs. (1), (2), (5), and (6), for the case of $\gamma_c \neq \gamma_v$, it can be shown that

$$\begin{aligned}\mathscr{J}(\hbar\omega) = {} & \frac{\gamma_c^2}{\sqrt{2e}} \exp\left(\frac{\hbar\omega - E_{g_o}}{\gamma_c}\right) \mathscr{Y}\left(\frac{\gamma_v}{2\gamma_c}\right) \\ & + \frac{1}{2\sqrt{e}} \frac{(\gamma_c\gamma_v)^{3/2}}{\gamma_v - \gamma_c} \left[\exp\left(\frac{\hbar\omega - E_{g_o} - \gamma_c/2}{\gamma_v}\right) \right. \\ & \left. - \exp\left(\frac{\hbar\omega - E_{g_o} - \gamma_v/2}{\gamma_c}\right) \right] \\ & + \frac{\gamma_v^2}{\sqrt{2e}} \exp\left(\frac{\hbar\omega - E_{g_o}}{\gamma_v}\right) \mathscr{Y}\left(\frac{\gamma_c}{2\gamma_v}\right),\end{aligned} \tag{A1}$$

where the function

$$\mathscr{Y}(z) \equiv \int_z^\infty \sqrt{x}\, \exp(-x)dx, \tag{A2}$$

which may be shown to be equal to

$$\mathscr{Y}(z) = \sqrt{z}\, \exp(-z) + \frac{\sqrt{\pi}}{2}\, \mathrm{erfc}(\sqrt{z}), \tag{A3}$$

the complimentary error function

$$\mathrm{erfc}(z) \equiv \frac{2}{\sqrt{\pi}} \int_z^\infty \exp(-x^2)dx. \tag{A4}$$

For the special case of $\gamma_c = \gamma_v = \gamma$, the second term of Eq. (A1) becomes

$$\frac{\gamma}{2e}\, \exp\left(\frac{\hbar\omega - E_{g_o}}{\gamma}\right)(E_{g_o} - \hbar\omega + \gamma), \tag{A5}$$

all other terms remaining unchanged. For the case of $\hbar\omega \geqslant E_{g_o} + \gamma_c/2 + \gamma_v/2$, from Eqs. (1), (2), (5), and (6), it can be shown that

$$\begin{aligned}\mathscr{I}(\hbar\omega) = {} & \frac{\gamma_c^2}{\sqrt{2e}}\, \exp\left(\frac{\hbar\omega - E_{g_o}}{\gamma_c}\right) \mathscr{Y}\left(\frac{\hbar\omega - E_{g_o}}{\gamma_c} - \frac{1}{2}\right) \\ & + (\hbar\omega - E_{g_o})^2 \mathscr{I}\left(\frac{\gamma_c}{2(\hbar\omega - E_{g_o})}, \frac{\gamma_v}{2(\hbar\omega - E_{g_o})}\right) \\ & + \frac{\gamma_v^2}{\sqrt{2e}}\, \exp\left(\frac{\hbar\omega - E_{g_o}}{\gamma_v}\right) \mathscr{Y}\left(\frac{\hbar\omega - E_{g_o}}{\gamma_v} - \frac{1}{2}\right),\end{aligned} \tag{A6}$$

where $\mathscr{Y}(\cdot)$ is as defined before, and

$$\mathscr{I}(x,y) \equiv \int_x^{1-y} \sqrt{z}\sqrt{1-z}dz. \tag{A7}$$

[1] G. D. Cody, ''Hydrogenated Amorphous Silicon,'' in *Semiconductors and Semimetals*, edited by J. I. Pankove (Academic, New York, 1984), Vol. 21B, p. 11.
[2] N. F. Mott and E. A. Davis, *Electronic Processes in Non-Crystalline Materials*, 2nd ed. (Clarendon, Oxford, 1979).
[3] N. F. Mott, Adv. Phys. **16**, 49 (1967).
[4] N. F. Mott, Philos. Mag. **17**, 1259 (1968).
[5] E. O. Kane, Phys. Rev. **131**, 79 (1963).
[6] B. I. Halperin and M. Lax, Phys. Rev. **148**, 722 (1966).
[7] J. L. Cardy, J. Phys. C **11**, L321 (1978).
[8] C. M. Soukoulis, M. H. Cohen, and E. N. Economou, Phys. Rev. Lett. **53**, 616 (1984).
[9] S. John, C. Soukoulis, M. H. Cohen, and E. N. Economou, Phys. Rev. Lett. **57**, 1777 (1986).
[10] Z.-Q. Zhang and P. Sheng, Phys. Rev. Lett. **57**, 909 (1986).
[11] M. Silver, L. Pautmeier, and H. Bässler, Solid State Commun. **72**, 177 (1989).
[12] M. Kemp and M. Silver, Appl. Phys. Lett. **62**, 1487 (1993).
[13] S. K. O'Leary, S. Zukotynski, and J. M. Perz, J. Appl. Phys. **72**, 2272 (1992).
[14] S. K. O'Leary, S. Zukotynski, and J. M. Perz, J. Appl. Phys. **78**, 4282 (1995).
[15] Support for a linear-exponential distribution of tail states comes from a number of different experimental results (Refs. 16–21). Unfortunately, none of these results are of sufficient resolution to rule out the possibility of other functional forms for the distribution of tail states. In fact, the more recent experimental results of Michiel *et al.* (Ref. 22), Street (Ref. 23), and Longeaud and Vanderhaghen (Ref. 24) suggest that substantial deviations from a linear-exponential distribution of tail states occur. However, the even more recent results of Aljishi *et al.* (Ref. 25) suggest that the distribution of tail states may be linear-exponential after all.
[16] T. Tiedje, J. M. Cebulka, D. L. Morel, and B. Abeles, Phys. Rev. Lett. **46**, 1425 (1981).
[17] T. Tiedje, ''Hydrogenated Amorphous Silicon,'' in *Semiconductors and Semimetals*, edited by J. I. Pankove (Academic, New York, 1984), Vol. 21C, p. 207.
[18] J. Orenstein and M. Kastner, Phys. Rev. Lett. **46**, 1421 (1981).
[19] H. Dersch, J. Stuke, and J. Beichler, Phys. Status Solidi B **105**, 265 (1981).
[20] M. Stutzmann and J. Stuke, Solid State Commun. **47**, 635 (1983).
[21] K. Winer and L. Ley, Phys. Rev. B **36**, 6072 (1987).
[22] H. Michiel, G. J. Adriaenssens, and E. A. Davis, Phys. Rev. B **34**, 2486 (1986).
[23] R. A. Street, Proc. SPIE **763**, 10 (1987).
[24] C. Longeaud and R. Vanderhaghen, Philos. Mag. B **61**, 277 (1990).
[25] S. Aljishi, J. D. Cohen, S. Jin, and L. Ley, Phys. Rev. Lett. **64**, 2811 (1990).
[26] It is noted that the transition point $V_c + \gamma_c/2$ is an inflection point in the DOS, i.e., $N_c(E)$ exhibits an upward curvature for $E < V_c + \gamma_c/2$, and a downward curvature for $E > V_c + \gamma_c/2$. The existence of an inflection point in the distribution of electronic states near the mobility edge was theoretically predicted by Zhang and Sheng (Ref. 10).
[27] D. A. Neamen, *Semiconductor Physics and Devices* (Irwin, Boston, 1992).
[28] Tiedje *et al.* (Ref. 16), interpreting the results of a similar time-of-flight experiment to necessarily yield a linear-exponential distribution of tail states, concluded that $\gamma_c = 27$ meV for high-quality hydrogenated amorphous silicon. Dersch *et al.* (Ref. 19) and Stutzmann and Stuke (Ref. 20) drew similar conclusions from electron-spin measurements of high-quality hydrogenated amorphous silicon. More recent total-yield photoelectron spectroscopy measurements on undoped hydrogenated amorphous silicon have found results of a similar magnitude, at room temperature, but it was noted that the conduction-band tail breadth parameter increased substantially with temperature (Ref. 25).
[29] Tiedje *et al.* (Ref. 16), Dersch *et al.* (Ref. 19), Stutzmann and Stuke (Ref. 20), and Aljishi *et al.* (Ref. 25), have results that are consistent with our determination of γ_v.
[30] The optical transition matrix element, $D^2(\hbar\omega)$, depends on many parameters. For a complete discussion, see Ley (Ref. 31), Jackson *et al.* (Ref. 32), and Street (Ref. 33).
[31] L. Ley, ''The Physics of Hydrogenated Amorphous Silicon II,'' in *Topics of Applied Physics*, edited by J. D. Joannopoulos and G. Lucovsky (Springer, New York, 1984), Vol. 56, p. 61.
[32] W. B. Jackson, S. M. Kelso, C. C. Tsai, J. W. Allen, and S.-J. Oh, Phys. Rev. B **31**, 5187 (1985).
[33] R. A. Street, *Hydrogenated Amorphous Silicon* (Cambridge, New York, 1991).
[34] S. K. O'Leary, S. Zukotynski, and J. M. Perz, Phys. Rev. B **52**, 7795 (1995).
[35] N. K. Hindley, J. Non-Cryst. Solids **5**, 17 (1970).
[36] C. H. Grein and S. John, Phys. Rev. B **39**, 1140 (1989).
[37] J. Tauc, R. Grigorovici, and A. Vancu, Phys. Status Solidi **15**, 627 (1966).
[38] J. Tauc, in *Amorphous and Liquid Semiconductors*, edited by J. Tauc (Plenum, New York, 1974), p. 159.
[39] R. V. Kruzelecky, D. Racansky, S. Zukotynski, and J. M. Perz, J. Non-Cryst. Solids **99**, 89 (1988).
[40] R. V. Kruzelecky, C. Ukah, D. Racansky, and S. Zukotynski, J. Non-Cryst. Solids **103**, 234 (1988).
[41] S. Adachi, J. Appl. Phys. **70**, 2304 (1991).
[42] G. D. Cody, J. Non-Cryst. Solids **141**, 3 (1992).
[43] G. D. Cody, T. Tiedje, B. Abeles, B. Brooks, and Y. Goldstein, Phys. Rev. Lett. **47**, 1480 (1981).
[44] C. B. Roxlo, B. Abeles, C. R. Wronski, G. D. Cody, and T. Tiedje, Solid State Commun. **47**, 985 (1983).
[45] P. D. Persans, A. F. Ruppert, S. S. Chan, and G. D. Cody, Solid State Commun. **51**, 203 (1984).
[46] Roxlo *et al.* (Ref. 44) found that E_o varies up to 25% when E^{**} is varied over 200 meV, indicating that the optical absorption spectrum of amorphous semiconductors is not exactly linear exponential in character.